Journal of
Composites Science

MDPI

Article

Optimization of Chitin Nanofiber Preparation by Ball Milling as Filler for Composite Resin

Dagmawi Abebe Zewude [1], Hironori Izawa [1,2,3] and Shinsuke Ifuku [1,2,*]

[1] Graduate School of Engineering, Tottori University, 4-101 Koyama-Minami, Tottori 680-8550, Japan; d19t3106x@edu.tottori-u.ac.jp (D.A.Z.); h-izawa@cc.miyazaki-u.ac.jp (H.I.)
[2] Center for Research on Green Sustainable Chemistry, Tottori University, Tottori 680-8550, Japan
[3] Faculty of Engineering, University of Miyazaki, 1-1 Gakuen Kibanadai-Nishi, Miyazaki 889-2192, Japan
* Correspondence: sifuku@tottori-u.ac.jp

Abstract: Chitin nanofiber is a nanomaterial produced by pulverizing chitin, the main component of crab shells. Since it has excellent mechanical properties, it is expected to be used as a reinforcing material to strengthen materials. Chitin was mechanically ground in water using a ball mill to prepare nanofibers. The ball size, total ball weight, and milling time were varied, and the resulting water dispersion and the cast film were analyzed to optimize the conditions for efficient preparation. The length and width of the nanofibers were also measured by SEM and AFM observations. The size of the balls affected the level of grinding and the intensity of impact energy on the chitin. The most efficient crushing was achieved when the diameter was 1 mm. The total ball weight directly affects the milling frequency, and milling proceeds as the total weight increases. However, if too many balls occupy the container, the grinding efficiency decreases. Therefore, a total ball weight of 300 g was optimal. Regarding the milling time, the chitin becomes finer depending on the increase of that time. However, after a specific time, the shape did not change much. Therefore, a milling time of approximately 150 min was appropriate.

Keywords: chitin nanofiber; ball milling; reinforcing material; nanocomposite

Citation: Zewude, D.A.; Izawa, H.; Ifuku, S. Optimization of Chitin Nanofiber Preparation by Ball Milling as Filler for Composite Resin. *J. Compos. Sci.* **2022**, *6*, 197. https://doi.org/10.3390/jcs6070197

Academic Editors: Yingtao Liu and Yirong Lin

Received: 15 June 2022
Accepted: 5 July 2022
Published: 6 July 2022

1. Introduction

Chitin is a polysaccharide with a chemical structure similar to cellulose with *N*-acetylglucosamine as the repeating unit. It is synthesized as a structural material by various organisms, including the outer shells of crabs, shrimp, and insects, and the cell walls of molds, mushrooms, and diatoms, and is known as the second most abundant biomass after cellulose. However, chitin is rarely used except for some medical materials, compared to the extensive industrial use of cellulose and its derivatives in paper, fiber, and food applications. This is because chitin is insoluble in common solvents, making it difficult to process. Using cellulose nanofiber production technology [1], we have developed a technology to prepare chitin nanofibers from crab shells [2]. Chitin nanofibers have a uniform shape with a width of approximately 10 nm and are easily processed because they are obtained as a uniform water dispersion. Several forms have been obtained by dehydration of aqueous dispersions of chitin nanofibers. For example, the threads have been produced by spinning [3], paper sheets by filtration [4], and sponges by freeze-drying [5]. Because it is a water dispersion, it is easier to evaluate its functionality, and in vitro and in vivo studies have revealed various physiological functions. For example, we have identified their effects when applied to the skin [6,7], taken [8,9], or administered to plants [10,11]. Utilizing those functions, healthcare-related products containing nanofibers have been commercialized. Other applications of chitin nanofibers include reinforcing fibers to strengthen materials, although carbon nanotubes are the major filler in nanocomposites [12,13]. Like cellulose nanofibers, chitin nanofibers are crystalline materials consisting of linear chitin molecules regularly arranged by hydrogen bonds and thus have excellent mechanical properties [14,15]. For this reason,

plastics composited with chitin nanofibers have been reported like cellulose nanofibers [16]. The reinforcing effect of chitin nanofibers significantly increased the plastic's strength and modulus of elasticity and reduced its thermal expansion [17]. In addition, the plastic maintained high transparency despite the high content of nanofibers. This is due to the size effect of nanofibers. When their width is sufficiently smaller than the wavelength of visible light, the light is hardly scattered in the composite.

Purified chitin can be mechanically pulverized in water to prepare chitin nanofibers. This is because the chitin in crab shells is composed of nanofibers [18]. That is, numerous chitin molecules assemble to form crystalline nanofibers. The chitin nanofibers form a complex with proteins, and their higher-order structures are organized as a crab shell. The voids are then filled with calcium carbonate. Since all-natural chitin exists as nanofibers, chitin from various sources such as shrimp shells [19] and mushrooms [20] can be converted to nanofibers. In addition, since natural chitin is an aggregate of nanofibers, chitin can be converted to nanofibers using a variety of milling machines. The nanofibers have been produced using a millstone grinder [21], a high-pressure homogenizer [22], and a high-speed blender [23]. These are breakdown-type methods in which micro-sized samples are pulverized and converted to nano. Compared to the so-called bottom-up method, in which chitin is dissolved and then regenerated to produce nano-chitin [24,25], the breakdown method is characterized by the fact that the naturally occurring crystalline nanostructure remains. Therefore, it is essential to note that the shape of the chitin nanofibers obtained depends on pulverization conditions, which can significantly change the physical properties of the dispersion and the molded product [26]. One of the typical milling machines is the ball mill. In a ball mill, hard balls are placed in a cylindrical container and rotated, causing the balls to move at high speed and grind the sample with impact and friction. Ball mill is relatively inexpensive, as milling machines have low energy consumption. The degree of milling can be easily controlled depending on conditions. It is a batch-type mill that can be used for milling small amounts. Therefore, the ball mill is expected to be one of the production devices for chitin nanofibers. Although there have been several related reports [27–29], there have been no studies on the direct preparation of aqueous dispersions of chitin nanofibers by wet processing using a ball mill. Therefore, to develop a new production method for chitin nanofibers, we attempted to produce chitin nanofibers by ball milling. Specifically, the optimal conditions for efficient production of chitin nanofibers were verified by milling with different ball sizes, total ball volume, and milling time, and analyzing the resulting milled fibers.

2. Materials and Methods

2.1. Materials

Chitin powder from crab shell was purchased from Koyo Chemicals Industry Co., Ltd., Sakaiminato, Japan and used as received. The degree of deacetylation was 6%.

2.2. Mechanical Milling of Chitin

Chitin was subjected to ball milling in Pulverisette 6 classic line (Fritsche Japan). The 60 g of chitin water dispersion (5 wt%) was put into a 500 mL zirconia container, and zirconia balls were added. Milling was performed at a rotation speed of 300 rpm and stopped every 30 min for 15 min for cooling. Different milling conditions were used to study the effect of these factors, including ball size (0.3–20 mm), total ball weight (20–600 g), and milling time (30–300 min). Specific milling conditions are summarized in Tables S1–S3, shown as the Supplementary Materials. After milling, balls were removed from chitin by decantation and were rinsed with distilled water to collect chitin.

2.3. Preparation of Chitin Nanofiber Cast Film

8 g of milled chitin dispersion (1 wt%) was mixed with 10 g of acetone and stirred for 1 h under low pressure to remove air bubbles. The resulting mixture was poured into

a Petri dish to dry at 35 °C for 36 h. Thus, obtained cast film was used to measure the transparency and density.

2.4. Characterization of Milled Chitin Dispersion and the Cast Film

The light transmittance of the milled chitin dispersion at a concentration of 0.1 wt% and the cast film was measured using a UV-Vis spectrophotometer (UV-2600i, Shimadzu Corporation, Kyoto, Japan). The spectra were recorded in the range of 300 to 900 nm.

The viscosity of the milled chitin dispersion at a concentration of 1 wt% was measured using Brookfield digital viscometer DV-E (Brookfield Engineering Laboratories, Middleboro, MA, USA) with spindle no. LV-3 and rotational speed of 6 rpm. The sample was kept in a water bath at a temperature of 30 °C for at least 45 min before measurement.

To study the amount of fully milled chitin, the chitin content in the supernatant was measured as nanofiber yield. After milling, the chitin dispersion was diluted to 0.1 wt% by water and centrifuged at 1000 rpm for 35 min to remove coarse microfiber, and concentrations before and after centrifugation were compared. The supernatant was also used for microscopic observation.

A field emission scanning electron microscope (FE-SEM, JSM-6701F, JEOL, Tokyo, Japan) was used to observe the morphology and measure the length of milled chitin. Before imaging, the sample was coated with an approximately 2 nm Pt layer using an ion sputter coater and observed at the electron-acceleration voltage of 2.0 kV. The fiber lengths of chitin nanofibers were determined by measuring over 150 randomly selected nanofibers from each sample.

An atomic force microscope (AFM, Nanocute, SII Instruments, Chiba, Japan) was also used to observe and measure the width of the nanofiber. The diluted sample was dropped on the freshly cleaved mica substrate and dried at 35 °C overnight for observation. The fiber widths were determined by measuring over 150 randomly selected points along the fiber axes.

The crystal structure was studied using an X-ray generator (Ultima IV, Rigaku Corporation, Tokyo, Japan) with Ni-filtered CuK_{α} radiation. The observation voltage and current were set at 40 kV and 40 mA, respectively. XRD sample was freeze-dried and then crushed using mortar and pestle. The crystallinity index (CI) was estimated from the X-ray profile using $CI = (I_{110} - I_{am}) \times 100/I_{110}$, where I_{110} is the maximum intensity of the 110 plane at approximately 19° and I_{am} is the amorphous diffraction intensity at 16° [30].

3. Results and Discussions

3.1. Influence of Ball Diameter

The optimum ball size for milling chitin was investigated. The total weight of the balls was fixed at 120 g and the grinding time at 120 min. Figure 1a shows the viscosity of the chitin dispersion when ground with balls of 0.3 to 20 mm in diameter. Viscosity correlates with the number of nanofibers produced by ball milling, specific surface area, and aspect ratio [26]. These parameters affect interactions such as intermolecular forces and physical entanglement between nanofibers. When the ball diameter was 20 mm, the viscosity was 150 mPa·s. The viscosity increased as the ball size decreased, reaching a maximum value of 300 mP·s at 1 mm. This was influenced by the specific surface area of the balls. For example, when the ball size changes from 20 mm to 5 mm, the number of balls with a total weight of 120 g increases from 5 to 286 balls, respectively, and their surface area increases significantly. As the container rotates on its own axis and orbits, the balls inside are up and down, and rotating at high speed. Then, balls collide with the chitin more frequently, resulting in more efficient grinding [31]. On the other hand, when the size was 0.3 mm, the viscosity decreased significantly to 140 mPa·s. The different result is presumably due to the impact force of the ball. The smaller ball size increases the surface area. In contrast, the lower weight per ball decreases the impact energy imparted to the sample, suggesting that the energy imparted by the 0.3 mm ball is insufficient for grinding chitin. Figure 1b shows the transparency of chitin dispersions milled with balls of different sizes. The

transparency of the dispersion is strongly influenced by the shape and dispersibility of the chitin nanofibers [26]. This is because well-milled chitin has a less diffuse reflection of visible light at the interface with water due to the nanosize effect. In addition, when the affinity between water molecules and nanofibers is high, aggregation between chitin is suppressed, and uniform dispersion is achieved, resulting in improved transparency. In Figure 1b, the transmittance increased continuously as the ball size decreased, suggesting that the chitin is more pulverized. This is because, as already mentioned, when the ball size is reduced, the frequency of collisions with the chitin increases, and the milling becomes more efficient. Figure 1c shows the yield of chitin nanofibers. Chitin contained in the supernatant solution of aqueous chitin dispersion after centrifugation was considered as nanofibers, and the yield was determined. Well-milled chitin nanofibers do not precipitate by centrifugation and remain in the supernatant because of their improved dispersibility in water. At a ball size of 20 mm, the yield of chitin nanofibers in the supernatant was 44% but increased with decreasing size, reaching 62% at 1 mm. At 0.3 mm, however, the percentage dropped to 45%. This trend agrees with that of viscosity since the impact by the 0.3 mm ball is insufficient to convert chitin into nanofibers, leaving coarse chitin fibers.

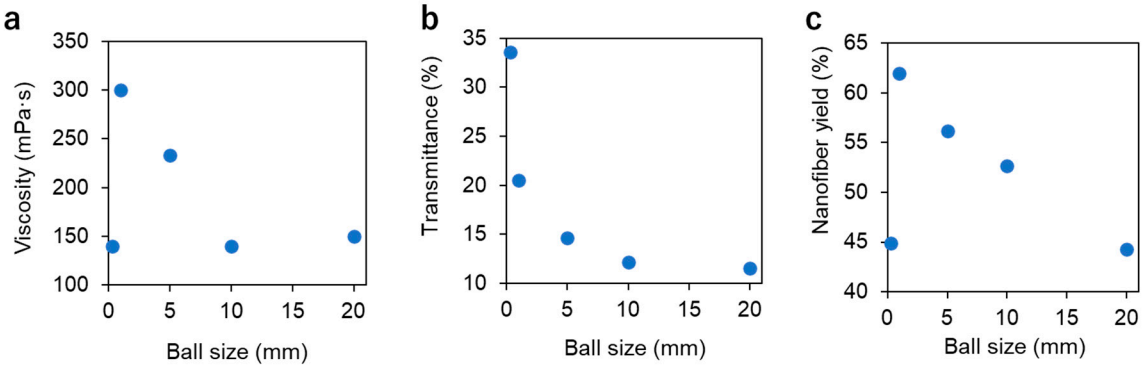

Figure 1. (**a**) Viscosity, (**b**) transmittance at 600 nm, and (**c**) nanofiber yield after milling of chitin using different ball sizes.

The transmittance at 600 nm and the density of cast films made with aqueous chitin nanofiber dispersion are shown in Figure 2. The transparency and density of the cast films are highly correlated with the degree of chitin pulverization [24,26]. Chitin is inherently a substance that absorbs little visible light, so its films can be transparent. Well-milled chitin nanofibers increase transmittance and density because they can be filled without gaps in the film after drying. On the other hand, coarse fibers with insufficient milling caused air voids in the film, thus reducing density. In addition, since air and chitin have very different refractive indices, a diffuse reflection of light occurs at the interface between them, reducing transparency. The results for transmittance and density of the cast film were in good agreement with those for the viscosity of the water dispersion and the percentage of supernatant. That is, the transmittance and density of the film increased as the ball size decreased, with the highest values at 1 mm. On the other hand, when the ball was 0.3 mm, the transmittance and density decreased. This supports the above discussion that ball size affects the frequency and grinding power of chitin grinding.

Milled chitin was observed by SEM and AFM (Figures S1 and S2). The distribution of nanofiber length and width obtained from the SEM and AFM images is shown in Figure 3. When the ball size was 1 mm, the distribution of nanofiber length was the narrowest, and the average fiber length was the smallest. That is, there were few nanofibers longer than 700 nm. Fibers with lengths between 100 and 300 nm accounted for 56% of the total. Regarding the distribution of nanofiber widths, chitin treated with 1 nm balls was the most pulverized. Fibers with widths greater than 13 nm were the least abundant (4%), and finer nanofibers with widths of less than 5 nm and 5–7 nm were the most abundant (13% and 34%, respectively).

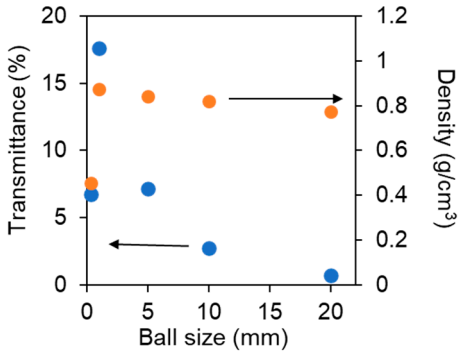

Figure 2. Dependence of transmittance at 600 nm (blue circle) and density (orange cercle) of the cast film on different ball sizes for milling of chitin.

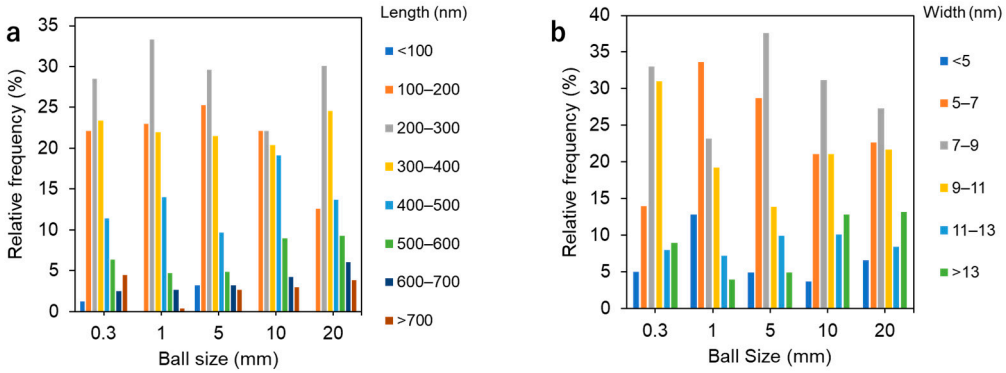

Figure 3. Distribution of (**a**) length and (**b**) width of chitin nanofibers milled at different ball sizes.

These results show that when grinding chitin in a ball mill, the size of the balls has a significant effect on the grinding of chitin. Reducing the size increases the ball's surface area, increasing the frequency of chitin grinding. On the other hand, if the balls are too small, they are too light and therefore insufficient for their crushing. Thus, the optimal ball size for crushing chitin is 1 mm.

3.2. Influence of Total Ball Weight

The optimal total ball weight for grinding chitin was investigated. Ball size and milling time were fixed at 1 mm and 120 min, respectively. The viscosities of the resulting aqueous chitin nanofiber dispersions are shown in Figure 4a when chitin was ground with balls with a total weight of 20 to 600 g. The viscosity, which was 140 mPa·s at a total ball weight of 20 g, increased as the ball weight increased, reaching a maximum value of 300 mPa·s at 120 g. This is because the total ball weight is proportional to the number of balls, thus increasing the frequency of chitin crushing. On the other hand, the viscosity decreased when the ball weight was above 300 g. This is presumably because excessive milling caused longitudinal cleavage parallel to the nano-fibrillation of the chitin, resulting in a decrease in aspect ratio. Shorter fibers decrease the viscosity of the dispersion. The transmittance of the nanofiber water dispersion is shown in Figure 4b. The transmittance was 15% when the total ball weight was 20 g and increased as the weight increased, reaching a maximum of 27% when the weight was 300 g. This is due to the increase in the number of balls and the frequency of milling, as well as the viscosity results. On the other hand, when the weight was 600 g, the transmittance decreased (16%). The grinding mechanism of a ball mill grinds the sample in a rotating container by impact and friction as the balls move against the inner walls of the container. When there is an excess of balls in the container, the motion of the balls is restricted and interferes with the grinding of the sample. Indeed, when using 600 g balls, the volume of balls in a 500 mL container is estimated to be 90 cm^3, accounting for 18%. That percentage is larger than that of the aqueous chitin dispersion. The results are similar

to the yield of chitin nanofibers remaining in the supernatant (Figure 4c). As the total weight of the balls increased, the percentage of chitin in the supernatant increased, reaching a maximum when the total weight was 300 g, with a yield of 75%. On the other hand, at 600 g, the yield decreased to 45%. Excess balls reduce the efficiency of the milling process.

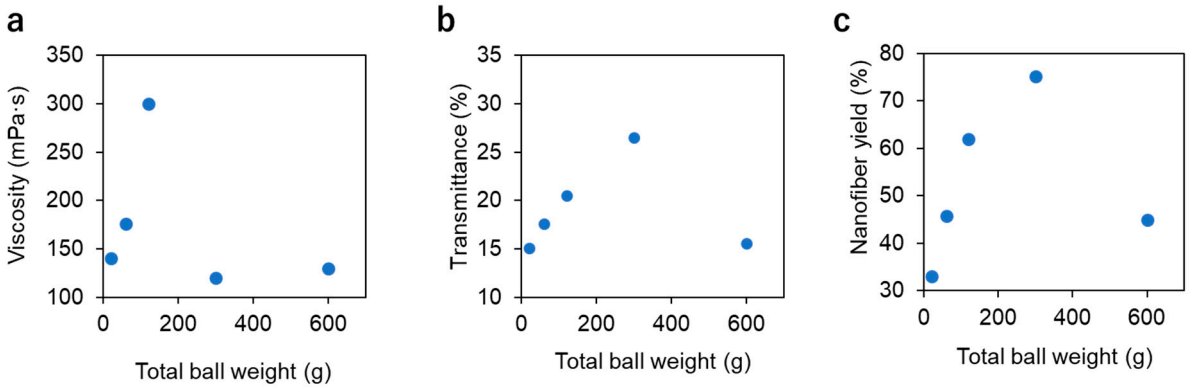

Figure 4. (**a**) Viscosity, (**b**) transmittance at 600 nm, and (**c**) nanofiber yield after milling of chitin using different total ball weights.

The transmittance and density of cast films prepared from aqueous nanofiber dispersion are shown in Figure 5. The trends in the transmittance and density of the films for different total ball weights correlate well with those of the aqueous dispersion. Specifically, as the total ball weight increased from 20 g to 300 g, the transmittance and density increased linearly from 2% to 55% and from 0.55 g/m^3 to 0.99 g/m^3, respectively. On the other hand, when the ball weight was 600 g from 300 g, they decreased to 9% and 0.75 g/m^3, respectively.

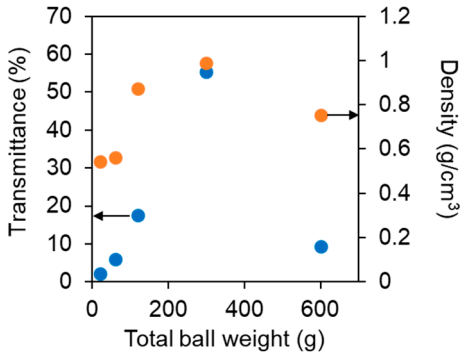

Figure 5. Dependence of transmittance at 600 nm (blue circle) and density (orange circle) of the cast film on different total ball weights for milling of chitin.

The distribution of length and width of nanofibers when milled with balls of different weights is shown in Figure 6. As the ball weight increased, the percentage of short nanofibers increased. For example, at a ball weight of 300 g, few fibers with lengths greater than 500 nm were present, while nanofibers with lengths of less than 100 nm and 100–200 nm were in the majority, at 11% and 36%, respectively. This indicates that the balls cut the nanofibers in the length direction. On the other hand, the width of the fibers tended to increase with ball weight. For example, when comparing the results for ball weights of 120 g, 300 g, and 600 g, the percentages of fibers with widths of 5–7 nm decreased to 33%, 17%, and 13%, respectively, while those with widths of 11 nm and above increased to 11%, 23%, and 31%. This may be due to changes in the crystallinity of chitin nanofibers.

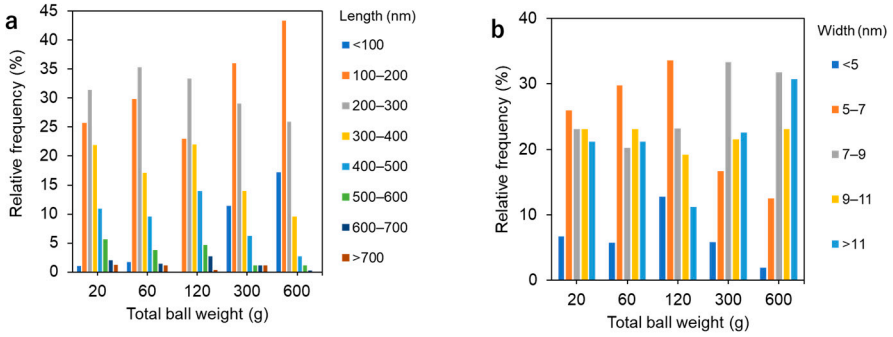

Figure 6. Distribution of (**a**) length and (**b**) width of chitin nanofibers milled at different total ball weights.

Therefore, to study the effect of total ball weight on the crystallinity of chitin, X-ray scattering measurements were performed, and the relative crystallinity was determined from the profiles (Figure 7). The crystallinity of the raw chitin was 90% but decreased with ball milling. The crystallinity decreased slowly with the total weight of the balls, and at a ball weight of 600 g, the crystallinity was 61%. This suggests that the ball impact is destroying the chitin crystals. Amorphization of crystalline chitin may be causing an increase in fiber width.

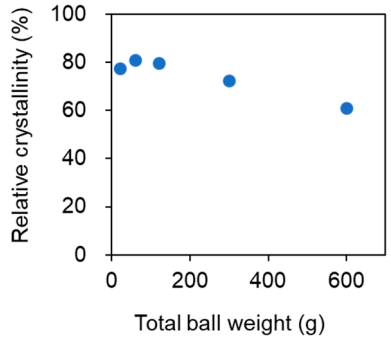

Figure 7. Dependence of relative crystallinity index of chitin nanofibers on total ball weight.

These results show that the total weight (or number) of balls significantly impacts chitin crushing. As the total weight increases, there are more opportunities for chitin to be crushed, resulting in increased fineness. However, when the vessel is filled with an excess of balls, the movement of the balls is inhibited, and thus the efficiency of the milling process is reduced. Therefore, the appropriate total weight of the balls under these milling conditions was 300 g.

3.3. Effect of Milling Time

The effect of grinding time by ball milling on chitin was investigated. Based on the results of the above study, the ball size and total ball weight were fixed at 1 mm and 300 g, respectively. The viscosity of the aqueous dispersion, when processed in the ball mill for 30 to 300 min, is shown in Figure 8a. The viscosity was highest at 200 mPa·s when the total milling time was 30 min. This is due to the conversion of chitin into nanofibers by milling, which increases the interaction between the fibers. On the other hand, after 60 min of grinding, the viscosity decreased significantly to 110 mPa·s, and the viscosity remained almost constant after further crushing. This suggests that the crushing process caused longitudinal cleavage parallel to the refinement of the chitin. A decrease in aspect ratio causes a decrease in viscosity. The transparency of the nanofiber dispersion is shown in Figure 8b. The light transmittance increased continuously with milling time. This suggests that the milling process refined the chitin fibers in the length and width directions, resulting in improved dispersion and suppression of optical scattering. However, after 240 min,

the transmittance had almost reached a plateau. The yield of chitin nanofibers in the supernatant of the dispersion is shown in Figure 8c. As the grinding time increased, the percentage of chitin increased significantly, reaching 75% after 120 min of grinding. After that, however, the increase in chitin yield became moderate. These results also suggest that the shape does not change significantly after a certain amount of milling time.

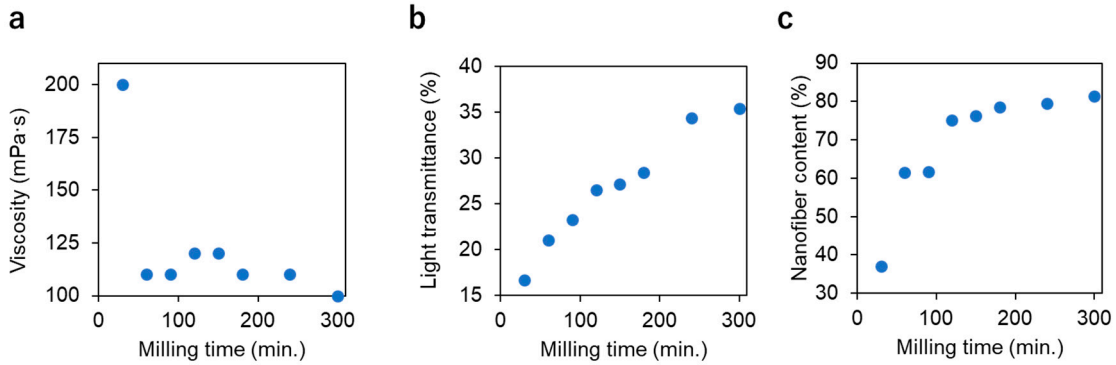

Figure 8. (**a**) Viscosity, (**b**) transmittance at 600 nm, and (**c**) nanofiber yield after milling of chitin with different milling times.

Such a trend of change in the physical properties of the nanofiber dispersion is also observed in the transmittance and density of its cast film (Figure 9). That is, the transmittance of the film increased with milling time. This suggests a progression of chitin refinement. The density of the film also increased with the progression. However, after 150 min of milling, the transmittance almost reached a plateau, and the same trend was observed for density.

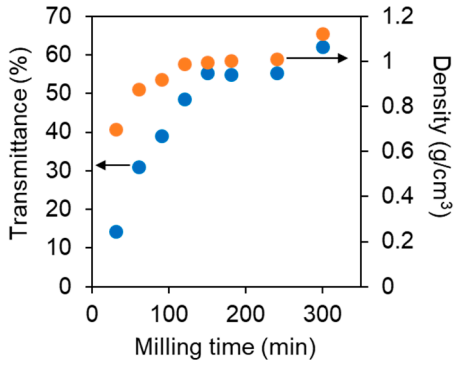

Figure 9. Dependence of transmittance at 600 nm (blue circle) and density (orange circle) of the cast film on milling time of chitin.

These results show that the nano-fibrillation of chitin progresses depending on the milling time, but the shape change converges after a certain amount of time. Therefore, the appropriate milling time was approximately 150 min.

4. Conclusions

Optimal conditions for producing chitin using a ball mill were identified. Ball size, total ball weight, and milling time significantly impact chitin milling efficiency. That is, the morphology of the nanofibers, the viscosity and transparency of their dispersions, and the yield of the nanofibers changed by them. The transparency and viscosity of their cast films also changed significantly depending on these milling conditions. Based on those results, the optimal conditions were determined to be a ball size of 1 mm, a total ball weight of 300 g, and a milling time of 150 min. Because of its excellent physical properties, chitin nanofiber is expected to be used as a reinforcing material to create nanocomposites.

Technology for efficiently grinding chitin into nanofibers using less energy is essential to promote the use of chitin nanofibers produced from underutilized resources.

Supplementary Materials: The following supporting information can be downloaded at: https://www.mdpi.com/article/10.3390/jcs6070197/s1, Figure S1: FE-SEM image of chitin nanofiber milled at a ball size of (a) 0.3, (b) 1, (c) 5, (d) 10, and (e) 20 mm; Figure S2: AFM image of chitin nanofiber milled at a ball size of (a) 0.3, (b) 1, (c) 5, (d) 10, and (e) 20 mm; Figure S3: FE-SEM image of chitin nanofiber milled at a ball weight of (a) 20, (b) 60, (c) 120, (d) 300, and (e) 600 g; Figure S4: AFM image of chitin nanofiber milled at a ball weight of (a) 20, (b) 60, (c) 120, (d) 300, and (e) 600 g; Figure S5: FE-SEM image of chitin nanofiber after milling for (a) 30, (b) 60, (c) 90, (d) 120, (e) 150, (f) 180 (g) 240, and (h) 300 min; Figure S6: AFM image of chitin nanofiber after milling for (a) 30, (b) 60, (c) 90, (d) 120, (e) 150, (f) 180 (g) 240, and (h) 300 min; Table S1: The weight and size of the milling ball and milling time used in each experiment for optimization of ball size; Table S2: The weight and size of the milling ball and milling time used in each experiment for optimization of total ball weight; Table S3: The weight and size of the milling ball and milling time used in each experiment for optimization of milling time.

Author Contributions: D.A.Z. conducted all experiments and analytical characterization. S.I. and H.I. conceived the presented idea and designed the research. D.A.Z. and S.I. contributed to writing the manuscript. All authors have read and agreed to the published version of the manuscript.

Funding: This research received no external funding.

Acknowledgments: D.A.Z. is very grateful for the scholarship from the Japanese ministry of education, culture, sports, science, and technology (MEXT).

Conflicts of Interest: The authors declare no conflict of interest.

References

1. Abe, K.; Iwamoto, S.; Yano, H. Obtaining cellulose nanofibers with a uniform width of 15 nm from wood. *Biomacromolecules* **2007**, *8*, 3276–3278. [CrossRef] [PubMed]
2. Ifuku, S.; Nogi, M.; Abe, K.; Yoshioka, M.; Morimoto, M.; Saimoto, H.; Yano, H. Preparation of chitin nanofibers with a uniform width as -chitin from crab shells. *Biomacromolecules* **2009**, *10*, 1584–1588. [CrossRef] [PubMed]
3. Das, P.; Heuser, T.; Wolf, A.; Zhu, B.; Demco, D.E.; Ifuku, S.; Walther, A. Tough and catalytically active hybrid biofibers wet-spun from nanochitin hydrogels. *Biomacromolecules* **2012**, *13*, 4205–4212. [CrossRef] [PubMed]
4. Ifuku, S.; Nogi, M.; Yoshioka, M.; Morimoto, M.; Yano, H.; Saimoto, H. Fibrillation of dried chitin into 10–20 nm nanofibers by a simple grinding method under acidic conditions. *Carbohydr. Polym.* **2010**, *81*, 134–139. [CrossRef]
5. Tan, A.; Zhou, X.; Wu, K.; Yang, D.; Jiao, Y.; Zhou, C. Tannic acid/Ca^{II} anchored on the surface of chitin nanofiber sponge by layer-by-layer deposition: Integrating effective antibacterial and hemostatic performance. *Int. J. Biol. Macromol.* **2020**, *159*, 304–315. [CrossRef] [PubMed]
6. Izumi, R.; Komada, S.; Ochi, K.; Karasawa, L.; Osaki, T.; Murahata, Y.; Tsuka, T.; Imagawa, T.; Itoh, N.; Okamoto, Y.; et al. Favorable effects of superficially deacetylated chitin nanofibrils on the wound healing process. *Carbohydr. Polym.* **2015**, *123*, 461–467. [CrossRef]
7. Azuma, K.; Koizumi, R.; Izawa, H.; Morimoto, M.; Saimoto, H.; Osaki, T.; Ito, N.; Yamashita, M.; Tsuka, T.; Imagawa, T.; et al. Hair growth-promoting activities of chitosan and surface-deacetylated chitin nanofibers. *Int. J. Biol. Macromol.* **2019**, *126*, 11–17. [CrossRef]
8. Goto, M.; Iohara, D.; Michihara, A.; Ifuku, S.; Azuma, K.; Kadowaki, D.; Maruyama, T.; Otagiri, M.; Hirayama, F.; Anraku, M. Effects of surface-deacetylated chitin nanofibers on non-alcoholic steatohepatitis model rats and their gut microbiota. *Int. J. Biol. Macromol.* **2020**, *164*, 659–666. [CrossRef]
9. Anraku, M.; Tabuchi, R.; Ifuku, S.; Nagae, T.; Iohara, D.; Tomida, H.; Uekama, K.; Maruyama, T.; Miyamura, S.; Hirayama, F.; et al. An oral absorbent, surface-deacetylated chitin nano-fiber amelioratesrenal injury and oxidative stress in 5/6 nephrectomized rats. *Carbohydr. Polym.* **2017**, *161*, 21–25. [CrossRef]
10. Egusa, M.; Matsui, H.; Urakami, T.; Okuda, S.; Ifuku, S.; Nakagami, H.; Kaminaka, H. Chitin nanofiber elucidates the elicitor activity of polymeric chitin in plants. *Front. Plant Sci.* **2015**, *6*, 1098. [CrossRef]
11. Parada, R.Y.; Egusa, M.; Aklog, Y.F.; Miura, C.; Ifuku, S.; Kaminaka, H. Optimization of nanofibrillation degree of chitin for induction of plant disease resistance: Elicitor activity and systemic resistance induced by chitin nanofiber in cabbage and strawberry. *Int. J. Biol. Macromol.* **2018**, *118*, 2185–2192. [CrossRef]
12. El Moumen, A.; Tarfaoui, M.; Nachtane, M.; Lafdi, K. Carbon nanotubes as a player to improve mechanical shockwave absorption. *Compos. B Eng.* **2019**, *164*, 67–71. [CrossRef]

13. Tarfaoui, M.; El Moumen, A.; Lafdi, K.; Hassoon, O.H.; Nachtane, M. Inter laminar failure behavior in laminate carbon nanotubes-based polymer composites. *J. Compos. Mater.* **2018**, *52*, 3655–3667. [CrossRef]
14. Vincent, J.; Wegst, U. Design and mechanical properties of insect cuticle. *Arthropod Struct. Dev.* **2004**, *33*, 187–199. [CrossRef] [PubMed]
15. Wada, M.; Saito, Y. Lateral thermal expansion of chitin crystals. *J. Polym. Sci. Part B Polym. Phys.* **2001**, *39*, 168–174. [CrossRef]
16. Ifuku, S.; Morooka, S.; Nakagaito, A.N.; Morimoto, M.; Saimoto, H. Preparation and characterization of optically transparent chitin nanofiber/(meth)acrylic resin composites. *Green Chem.* **2011**, *13*, 1708–1711. [CrossRef]
17. Ifuku, S.; Ikuta, A.; Egusa, M.; Kaminaka, H.; Izawa, H.; Morimoto, M.; Saimoto, H. Preparation of high-strength transparent chitosan film reinforced with surface-deacetylated chitin nanofibers. *Carbohydr. Polym.* **2013**, *98*, 1198–1202. [CrossRef]
18. Raabe, D.; Romano, P.; Sachs, C.; Fabritius, H.; Al-Sawalmih, A.; Yi, S.B.; Servos, G.; Hartwig, G.G. Microstructure and crystallographic texture of the chitin–protein network in the biological composite material of the exoskeleton of the lobster *Homarus americanus*. *Mater. Sci. Eng. A* **2006**, *421*, 143–153. [CrossRef]
19. Ifuku, S.; Nogi, M.; Abe, K.; Yoshioka, M.; Morimoto, M.; Saimoto, H.; Yano, H. Simple preparation method of chitin nanofibers with a uniform width of 10–20nm from prawn shell under neutral conditions. *Carbohydr. Polym.* **2011**, *84*, 762–764. [CrossRef]
20. Ifuku, S.; Nomura, R.; Morimoto, M.; Saimoto, H. Preparation of chitin nanofibers from mushrooms. *Materials* **2011**, *4*, 1417–1425. [CrossRef]
21. Ifuku, S.; Morooka, S.; Morimoto, M.; Saimoto, H. Acetylation of chitin nanofibers and their transparent nanocomposite films. *Biomacromolecules* **2010**, *11*, 1326–1330. [CrossRef] [PubMed]
22. Ifuku, S.; Yamada, K.; Morimoto, M.; Saimoto, H. Nanofibrillation of dry chitin powder by star burst system. *J. Nanomater.* **2012**, *2012*, 645624. [CrossRef]
23. Zewude, D.A.; Izawa, H.; Ifuku, S. Optimum preparation conditions for highly individualized chitin nanofibers using ultrasonic generator. *Polymers* **2021**, *13*, 2501. [CrossRef] [PubMed]
24. Zewude, D.A.; Noguchi, T.; Sato, K.; Izawa, H.; Ifuku, S. Production of chitin nanoparticles by bottom-up approach from alkaline chitin solution. *Int. J. Biol. Macromol.* **2022**, *210*, 123–127. [CrossRef] [PubMed]
25. Shams, M.I.; Ifuku, S.; Nogi, M.; Oku, T.; Yano, H. Fabrication of optically transparent chitin nanocomposites. *Appl. Phys. A* **2011**, *102*, 325–331. [CrossRef]
26. Dutta, A.K.; Yamada, K.; Izawa, H.; Morimoto, M.; Saimoto, H.; Ifuku, S. Preparation of chitin nanofibers from dry chitin powder by star burst system: Dependence on number of passes. *J. Chitin Chitosan Sci.* **2013**, *1*, 59–64. [CrossRef]
27. Liu, L.; Chenhuang, J.; Lu, Y.; Fan, Y.; Wang, Z. Facile preparation of nanochitins via acid assisted colloid milling in glycerol. *Cellulose* **2020**, *27*, 6935–6944. [CrossRef]
28. Tran, T.H.; Nguyen, H.; Hao, L.T.; Kong, H.; Park, J.M.; Jung, S.; Cha, H.G.; Lee, J.Y.; Kim, H.; Hwan, S.Y.; et al. A ball milling-based one-step transformation of chitin biomass to organo-dispersible strong nanofibers passing highly time and energy consuming processes. *Int. J. Biol. Macromol.* **2019**, *125*, 660–667. [CrossRef]
29. Zhong, T.; Wolcott, M.P.; Liu, H.; Glandon, N.; Wang, J. The influence of pre-fibrillation via planetary ball milling on the extraction and properties of chitin nanofibers. *Cellulose* **2020**, *27*, 6205–6216. [CrossRef]
30. Zhang, Y.; Xue, C.; Xue, Y.; Gao, R.; Zhang, X. Determination of the degree of deacetylation of chitin and chitosan by X-ray powder diffraction. *Carbohydr. Res.* **2005**, *340*, 1914–1917. [CrossRef]
31. Shin, H.; Lee, S.; Jung, H.S.; Kim, J. Effect of ball size and powder loading on the milling efficiency of a laboratory-scale wet ball mill. *Ceram. Int.* **2013**, *39*, 8963–8968. [CrossRef]